A Simple Broad-Band Device De-embedding Method Using an Automatic Network Analyzer with Time-Domain Option

GREGOR GRONAU AND INGO WOLFF, FELLOW, IEEE

Abstract—**A simple method for de-embedding S parameters of devices in microstrip is presented. The use of only one transmission line and two nonideal shorts or opens different in length as calibration standards allows the determination of the unknown S parameters of the connectors and the complex propagation coefficient of the lines.**

I. Introduction

THE ACCURATE measurement of a device embedded in a microstrip line requires a calibration process for the automatic network analyzer (ANA). An overview of the possible calibration and de-embedding techniques is given in [1]. All these methods use the actual S parameters measured directly in the frequency domain by the ANA. In contrast to these methods, this paper will illustrate (as in [2] for one-port measurements) that the use of the time-domain option implemented in the ANA HP 8510 or WILTRON 360 leads to a simple and quite accurate two-port de-embedding method in the frequency range 1–25 GHz. The calibration standards used in this technique are one transmission line and an element with a reflection coefficient $|\Gamma|$ near 1 (e.g., open or shortened ends). It should be mentioned that theoretically this element may be arbitrary, because the procedure will determine the value of Γ, as shown later.

In the first step the ANA must be calibrated with the available standards so that the subsequent measurements will give the correct S parameters at ports 1 and 2 of the ANA (Fig. 1). Taking into account that reflections on the microstrip lines due to small losses are negligible, the signal flowchart representation of the complete test fixture with the device under test (DUT) shown in Fig. 1 is valid and can be used to determine all unknown elements necessary for the de-embedding process. The figure shows the signal flowchart of the device under test characterized by S_{11}, S_{12}, S_{21}, and S_{22}. The elements A_{11}, A_{12}, A_{21}, A_{22}, B_{11}, B_{12}, B_{21}, and B_{22} represent the S parameters of the connectors 1 and 2 which are necessary to connect the

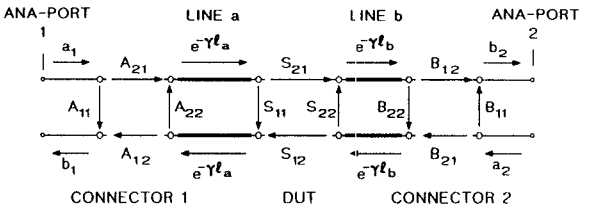

Fig. 1. Signal flowchart of the complete test fixture with DUT.

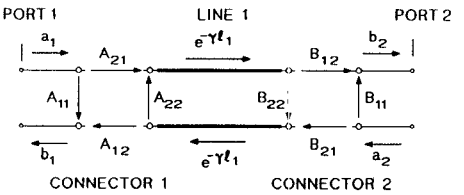

Fig. 2. Signal flowchart of the test fixture with a transmission line of length l_1.

stripline to the coaxial line of the ANA. The reference planes of the connectors are given by the reference planes of the calibration standards on the coaxial side and by the beginning of the microstrip line on the opposite side. Here γ is the propagation coefficient of the dominant quasi-TEM mode on the microstrip lines. Because of the reciprocity of the connectors used, the S parameters A_{12}, A_{21} and B_{12}, B_{21}, respectively, are equal and will be called A or B in the following ($A_{12} = A_{21} = A$ and $B_{12} = B_{21} = B$).

II. Measurements Using the Time-Domain Option [3], [4]

In a first measurement cycle both connectors are connected to a microstrip transmission line, as shown in Fig. 2. The length l_1 of this line must be chosen so that there is no interaction between the reflections of the two connectors in the time domain, as outlined in Fig. 3. This figure shows the measured reflection coefficient S_{11} at port 1 in the time domain. The measured reflection of connector 1 caused by the transition between the coaxial and microstrip lines appears earlier (≈ 0 ns) than the reflection from connector 2 (≈ 0.59 ns) caused by the transition from microstrip to coaxial line. If the distance between the reflections produced by different objects is large enough, this means that there is no interaction between the reflec-

Manuscript received November 5, 1987; revised September 30, 1988.

G. Gronau was with the Department of Electrical Engineering, Duisburg University, D-4100 Duisburg, West Germany. He is now with ArguMens GmbH, D-4100 Duisburg 1, West Germany.

I. Wolff is with the Department of Electrical Engineering and Sonderforschungsbereich 254, Duisburg University, D-4100 Duisburg 1, West Germany.

IEEE Log Number 8825390.

0018-9480/89/0300-0479$01.00 ©1989 IEEE

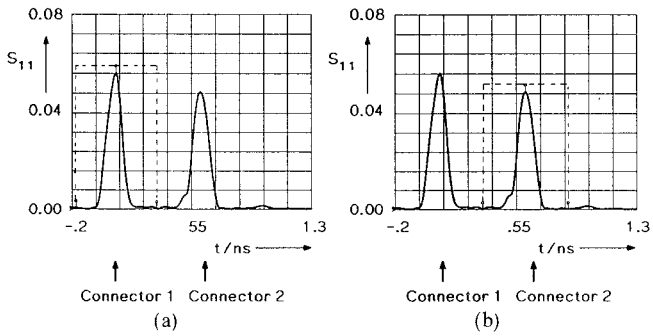

Fig. 3. Time-domain response at port 1 and appropriate gates for gating out the reflections of the connectors. (a) Gate on the first reflection. (b) Gate on the second reflection.

tions in the time domain, and each reflection may be measured separately. This is carried out by centering a gate with the correct gate span on the first reflection in the time domain, as outlined in Fig. 3(a), and the gating is switched on. This means that all reflections *outside* the gate are set to zero.

Transforming the time-domain results achieved by gating at ports 1 and 2, respectively, into the frequency domain delivers the measured values of A_{11} and B_{11} directly.

$$A_{11} \quad \text{and} \quad B_{11}.$$

Placing the gate on the second reflection as shown in Fig. 3(b), which is caused by the opposite connector, the following reflections are measured at port 1 and port 2, respectively:

$$A^2 B_{22} e^{-2\gamma l_1} = S_{22B} \tag{1}$$

$$B^2 A_{22} e^{-2\gamma l_1} = S_{22A}. \tag{2}$$

Measurement of the signal transmitted from port 1 to port 2 "gated out" by a suitable gate gives

$$S_{21L1} = S_{12L1} = ABe^{-\gamma l_1}. \tag{3}$$

In the next steps the transmission line in Fig. 2 is replaced by two open-ended lines of length l_2 and l_3, respectively. The measurement of the reflection coefficient Γ at the ends of the two lines, by centering the gate on the reflection from this element, leads to the measured values S_{11RL2}, S_{22RL2}, S_{11RL3}, and S_{22RL3}:

$$A^2 \Gamma e^{-2\gamma l_2} = S_{11RL2} \tag{4}$$

$$B^2 \Gamma e^{-2\gamma l_2} = S_{22RL2} \tag{5}$$

$$A^2 \Gamma e^{-2\gamma l_3} = S_{11RL3} \tag{6}$$

and

$$B^2 \Gamma e^{-2\gamma l_3} = S_{22RL3}. \tag{7}$$

Combining (4) and (7), the propagation coefficient γ is determined as

$$\gamma = \frac{1}{2(l_2 - l_3)} \ln\left\{\frac{1}{2}\left[\frac{S_{11RL3}}{S_{11RL2}} + \frac{S_{22RL3}}{S_{22RL2}}\right]\right\}. \tag{8}$$

Equations (4), (5), and (8) give the reflection coefficient of the open or short line as

$$\Gamma^2 = \frac{S_{11RL2} S_{22RL2} e^{4\gamma l_2}}{(AB)^2}. \tag{9}$$

Using (3) and replacing (AB) in (9) by

$$(AB)^2 = S_{21L1}^2 e^{-2\gamma l_1} \tag{10}$$

the unknown reflection coefficient Γ is finally determined as

$$\Gamma = \frac{(S_{11RL2} S_{22RL2})^{1/2}}{S_{21L1}} e^{\gamma(2l_2 - l_1)}. \tag{11}$$

From (4), (5), (1), and (2) the remaining scattering parameters of the connectors in Fig. 1 are calculated as

$$A = \left[\frac{S_{11RL2}}{\Gamma}\right]^{1/2} e^{\gamma l_2} \qquad B = \left[\frac{S_{22RL2}}{\Gamma}\right]^{1/2} e^{\gamma l_2}$$

$$A_{22} = \frac{S_{22A}}{B^2} e^{2\gamma l_1} \qquad B_{22} = \frac{S_{22B}}{A^2} e^{2\gamma l_1}. \tag{12}$$

For de-embedding the DUT, the scattering matrices $\vec{S}_1$ and $\vec{S}_2$ representing the connectors 1 and 2 are written in the form

$$\vec{S}_1 = \begin{bmatrix} A_{11} & A \\ A & A_{22} \end{bmatrix} \quad \text{and} \quad \vec{S}_2 = \begin{bmatrix} B_{22} & B \\ B & B_{11} \end{bmatrix}. \tag{13}$$

Using the scattering matrices of line a and line b ($\vec{S}_{La}$, $\vec{S}_{Lb}$) in Fig. 1 and calculating the chain-scattering matrices $\vec{K}_{La}$, $\vec{K}_{Lb}$, $\vec{K}_1$, and $\vec{K}_2$ of $\vec{S}_{La}$, $\vec{S}_{Lb}$, $\vec{S}_1$, and $\vec{S}_2$, the chain-scattering matrix $\vec{K}$ of the DUT is given by

$$\vec{K} = \vec{K}_{La}^{-1} \vec{K}_1^{-1} \vec{K}_m \vec{K}_2^{-1} \vec{K}_{Lb}^{-1} \tag{14}$$

where $\vec{K}_m$ is the chain-scattering matrix of the network between port 1 and port 2 in Fig. 1. $\vec{K}_m$ is calculated from the measured scattering matrix $\vec{S}_m$.

III. Applications

To demonstrate the usefulness of the technique, first the results for the propagation coefficient and the reflection coefficient of an open-ended microstrip line derived from (8) and (11) are compared with theoretical results. From the measurements described in Section II it is found that the relative error in determining the effective dielectric constant ϵ_{eff} from measurement in comparison with the results obtained from the expressions presented in [5] is less than 1 percent in the frequency range of interest.

The possibility of determining the calibration object during the calibration process by using (11) is outlined in Figs. 4 and 5. Comparison of the measured and calculated [6] open end effect on two different substrate materials ($\epsilon_r = 2.2$ and $\epsilon_r = 9.9$) yields good agreement for the substrates under test. Only at frequencies higher than 15 GHz is a deviation between measurement and theory observed. This deviation is due to the incorrectness of the model for the open end effect described in [6]. If a full-wave frequency-dependent model is used, the deviations between

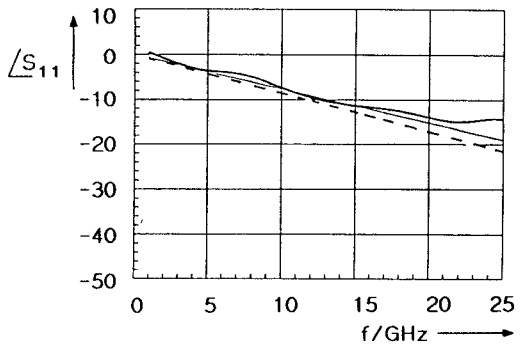

Fig. 4. Theoretical and measured phase of S_{11} of an open end in microstrip technique ($Z_L = 50\ \Omega$, $\epsilon_r = 2.2$, $h = 0.508$ mm). —— measurement; —— spectral-domain result; ---- [6].

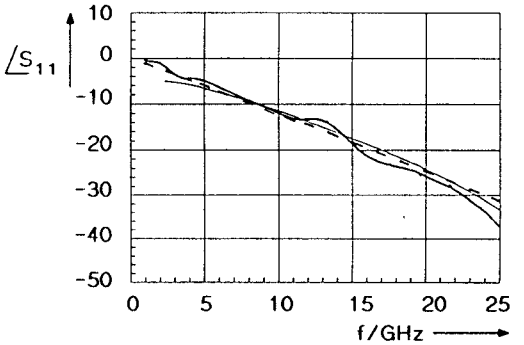

Fig. 5. Theoretical and measured phase of S_{11} of an open end in microstrip technique ($Z_L = 50\ \Omega$, $\epsilon_r = 9.9$, $h = 0.635$ mm). —— measurement; —— spectral domain result; ---- [6].

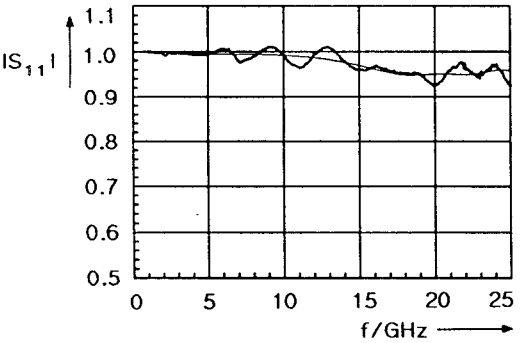

Fig. 6. $|S_{11}|$ of an open end ($l_a = 29.406$ mm, $Z_L = 50\ \Omega$, $\epsilon_r = 2.2$, $h = 0.508$ mm). —— frequency-domain measurement; —— result from (11).

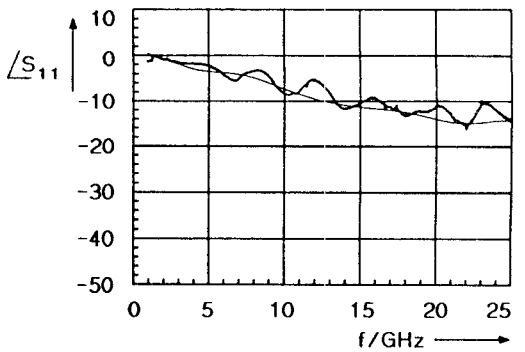

Fig. 7. $\angle S_{11}$ of an open end ($l_a = 29.406$ mm, $Z_L = 50\ \Omega$, $\epsilon_r = 2.2$, $h = 0.508$ mm). —— frequency-domain measurement; —— result from Fig. 4.

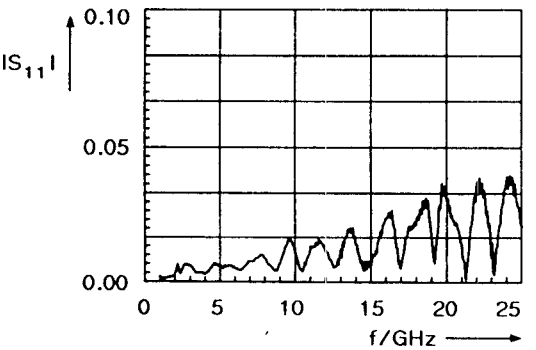

Fig. 8. Measured $|S_{11}|$ of a transmission line of zero length ($Z_L = 50\ \Omega$, $l_a = l_b = 25.4$ mm, $\epsilon_r = 2.2$, $h = 0.508$ mm).

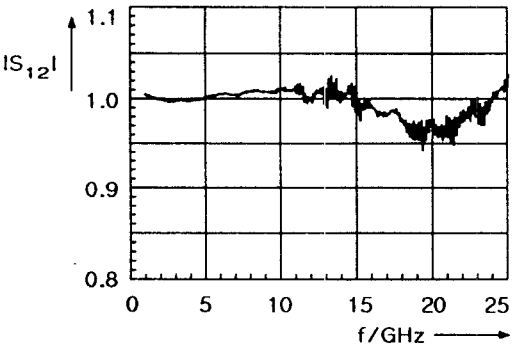

Fig. 9. Measured $|S_{12}|$ of a transmission line of zero length ($Z_L = 50\ \Omega$, $l_a = l_b = 25.4$ mm, $\epsilon_r = 2.2$, $h = 0.508$ mm).

theory and experiment are smaller, even at higher frequencies.

Using the results for describing the S parameters of the connectors, assuming reproducibility of the connections, and applying the derived equations, the method was used to measure different test objects. This is achieved by measuring the S parameters at test ports 1 and 2 of the ANA in the frequency domain and then using (14) for de-embedding.

Figs. 6 and 7 show the results of the de-embedding process for a microstrip open end. To compare these results with those from (11) the values are additionally plotted in Figs. 6 and 7. Comparison of the results shows a good agreement for this element and outlines a measurement accuracy of $\pm 5°$ for the phase angle.

Another example to demonstrate the validity of the technique is illustrated in Figs. 8, 9, and 10. The DUT is a transmission line of length $l = 50.8$ mm. Transforming the measured results in a reference plane lying in the middle of the substrate using $l_a = l_b = l/2$ (see Fig. 1), the expected results for the scattering parameters are those of a through-connection: $S_{11} = S_{22} = 0$ and $S_{12} = S_{21} = 1$.

The measurement of this ideal element offers the possibility of discussing the accuracy of the procedure more precisely. From Figs. 8 and 9 the maximum difference between the expected and measured results for the absolute values of the scattering parameters is determined to be 0.05. It must be mentioned that this accuracy is achieved

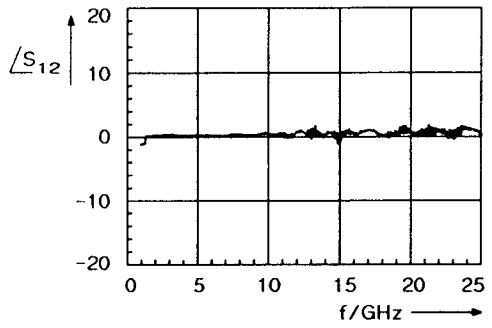

Fig. 10. Measured $\angle S_{12}$ of a transmission line of zero length (Z_L = 50 Ω, $l_a = l_b = 25.4$ mm, $\epsilon_r = 2.2$, $h = 0.508$ mm).

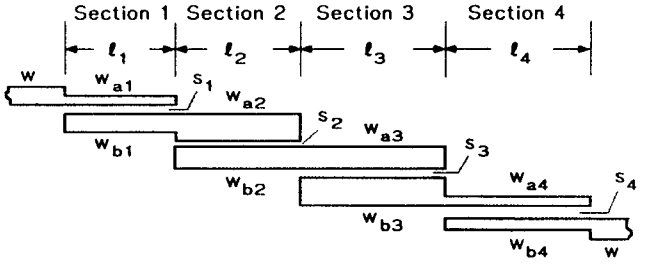

Fig. 11. Geometry of a coupled line filter in microstrip technique used as test object.

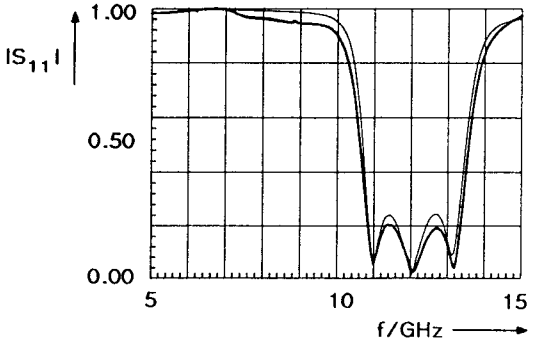

(a)

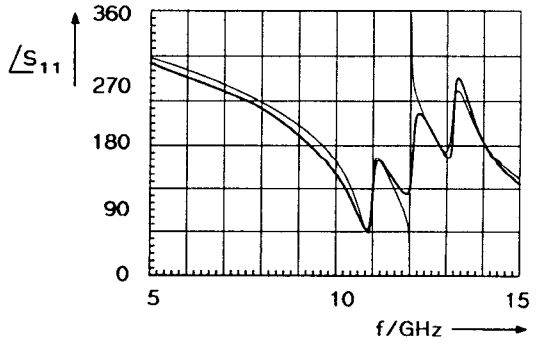

(b)

Fig. 12. Measured (——) and calculated (——) S_{11} of the filter in Fig. 11. (a) magnitude; (b) phase angle ($l_1 = 4.612$ mm, $l_2 = 4.519$ mm, $l_3 = 4.502$ mm, $l_4 = 4.599$ mm, $w_{a1} = 0.815$ mm, $w_{b1} = 0.331$ mm, $w_{a2} = 0.387$ mm, $w_{b2} = 0.381$ mm, $w_{a3} = 0.380$ mm, $w_{b3} = 0.393$ mm, $w_{a4} = 0.329$ mm, $w_{b4} = 0.806$ mm, $s_1 = 0.100$ mm, $s_2 = 0.340$ mm, $s_3 = 0.325$ mm, $s_4 = 0.101$ mm, $w = 1.580$ mm, $h = 0.508$ mm, $\epsilon_r = 2.2$).

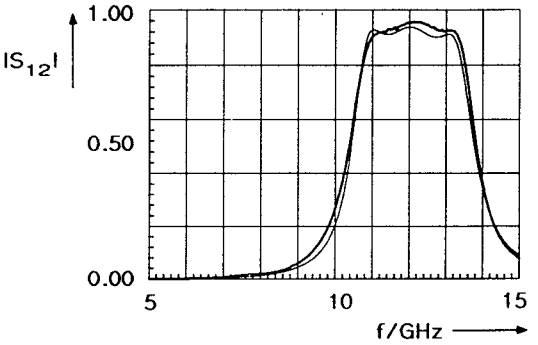

(a)

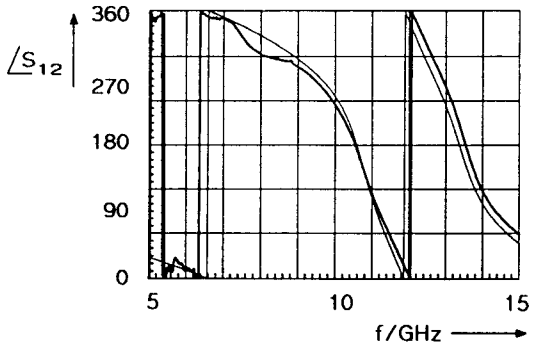

(b)

Fig. 13. Measured (——) and calculated (——) S_{12} of the filter in Fig. 11. (a) magnitude; (b) phase angle ($l_1 = 4.612$ mm, $l_2 = 4.519$ mm, $l_3 = 4.502$ mm, $l_4 = 4.599$ mm, $w_{a1} = 0.815$ mm, $w_{b1} = 0.331$ mm, $w_{a2} = 0.387$ mm, $w_{b2} = 0.381$ mm, $w_{a3} = 0.380$ mm, $w_{b3} = 0.393$ mm, $w_{a4} = 0.329$ mm, $w_{b4} = 0.806$ mm, $s_1 = 0.100$ mm, $s_2 = 0.340$ mm, $s_3 = 0.325$ mm, $s_4 = 0.101$ mm, $w = 1.580$ mm, $h = 0.508$ mm, $\epsilon_r = 2.2$).

by taking into account the measured frequency dependence of the propagation coefficient, the open ended line, and the scattering parameters of the connectors. There are no assumptions on the characteristic impedance or on the connectors used during the whole process. The result presented for the measured phase angle of the through-connection (Fig. 10), indicating only small differences between theory and experiment, gives further information concerning the usefulness and achievable measurement accuracy of this "user friendly" method.

In a last example a coupled microstrip line filter with unequal line widths in the coupled line sections as shown in Fig. 11 is used as the DUT. For comparison the measured and the theoretically calculated (achieved by using the software package OCTOPUS [7]) reflection and transmission coefficients (magnitude and phase angle) are plotted in Fig. 12 and Fig. 13. The agreement between the theoretical and measured results is very good. This is true even for the phase angles, which normally are difficult to calculate and measure.

IV. Conclusions

A simple *broad-band* *S*-parameter measurement method is presented. The use of the time-domain option allows the determination of the calibration standards and the unknown scattering parameters of the transitions connecting

the microstrip line to the coaxial measurement system of the ANA. It should be mentioned that the procedure presented is also applicable to other waveguide systems which satisfy the assumptions mentioned above. Knowing these parameters, the use of (14) leads to the S parameters of the DUT embedded in a microstrip line. The usefulness of the method is demonstrated by measured S parameters of microstrip structures, which show a very good agreement between the de-embedded measured and the expected theoretical results. Using the de-embedding technique, it is assumed that test fixtures are available which can reproducibly be remounted. As investigations of the authors show, carefully designed and produced test fixtures should have a reproducibility accuracy of 0.05 in magnitude and 5° in phase angle. Under these conditions the measurement accuracy mentioned above can be reached using the described calibration and de-embedding technique.

REFERENCES

[1] R. Lane, "De-embedding device scattering parameters," *Microwave J.*, vol. 27, pp. 149–156, Aug. 1984.

[2] M. E. Hines and H. E. Stinehelfer, "Time-domain oscillographic microwave network analysis using frequency-domain data," *IEEE Trans. Microwave Theory Tech.*, vol. MTT-22, pp. 276–282, Mar. 1974.

[3] Hewlett-Packard Co., "Real-time measurements in wideband network analyser," *Microwave J.*, vol. 27, pp. 139–145, Jan. 1984.

[4] F. J. Harris, "On the use of windows for harmonic analysis with the discrete fourier transform," *Proc. IEEE*, vol. 66, pp. 51–83, Jan. 1978.

[5] M. Kirschning and R. H. Jansen, "Accurate model for the effective dielectric constant of microstrip with validity up to millimeterwave frequencies," *Electron. Lett.*, vol. 18, pp. 272–273, 1982.

[6] N. H. L. Koster, R. H. Jansen, and M. Kirschning, "Accurate model for the open end effect of microstrip line," *Electron. Lett.*, vol. 17, pp. 532–535, 1981.

[7] OCTOPUS: MIC-design program of ArguMens Mikrowellenelektronik GmbH, Bismarckstr. 67, D-4100 Duisburg, FRG.

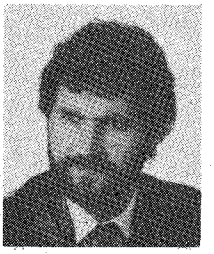

Gregor Gronau was born in 1957. He studied electrical engineering at Duisburg University, West Germany, from 1977 to 1983. In 1987 he received the doctoral degree with a dissertation on microstrip antennas. His main research activities include printed antennas, microstrip circuit design, and S-parameter measurement techniques.

Currently he is developing microstrip circuit design tools at the ArguMens GmbH, Duisburg, West Germany.

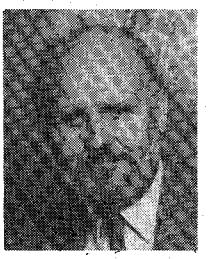

Ingo Wolff (M'75–SM'85–F'88) was born in 1938. He studied electrical engineering at the Technical University, Aachen, West Germany, from 1958 to 1964. In Aachen he received the doctoral degree (1967) and the Habilitation degree (1970) in high-frequency techniques.

From 1970 to 1974, he was an Associate Professor for High Frequency Techniques at the Technical University of Aachen. Since 1974, he has been a Full Professor of Electromagnetic Field Theory at Duisburg University, Duisburg, West Germany. His main research interests have been electromagnetic field theory in isotropic and anisotropic materials and their applications in planar microwave and millimeter-wave circuits. Since 1986 he has been leading a research group for MMIC techniques with 50 scientists at Duisburg University.